Published in final edited form as:
Am J Respir Cell Mol Biol. 2003 July ; 29(1): 106–116. doi:10.1165/rcmb.2002-0241OC.

Cytokine–Chemokine Networks in Experimental Mycobacterial and Schistosomal Pulmonary Granuloma Formation

Bo-Chin Chiu, **Christine M. Freeman**, **Valerie R. Stolberg**, **Eric Komuniecki**, **Pamela M. Lincoln**, **Steven L. Kunkel**, and **Stephen W. Chensue**
Department of Pathology, University of Michigan Medical School; and the Department of Pathology and Laboratory Medicine, Veterans Affairs Healthcare System, Ann Arbor, Michigan

Abstract

Type-1 and type-2 lung granulomas, respectively, elicited by bead immobilized *Mycobacteria bovis* and *Schistosoma mansoni* egg antigens (Ags) display different patterns of chemokine expression. This study tested the hypothesis that chemokine expression patterns were related to upstream cytokine signaling. Using quantitative transcript analysis, we defined expression profiles for 16 chemokines and then examined the *in vivo* effects of neutralizing antibodies against interferon-γ (IFN-γ), interleukin (IL)-4, IL-10, IL-12, and IL-13. Transcripts for CXCL2, −5, −9, −10, and −11 and the CCL chemokine, CCL3, and lymphotactin (XCL1), were largely enhanced by Th1-related cytokines, IFN-γ or IL-12. Transcripts for CCL11, CCL22, CCL17, and CCL1 were enhanced largely by Th2-related cytokines, IL-4, IL-10, or IL-13. Transcripts for CCL4, CCL2, CCL8, CCL7, and CCL12 were potentially induced by either Th1- or Th2-related cytokines, although some of these showed biased expression. IFN-γ and IL-4 enhanced the greatest complement of transcripts, and their neutralization had the greatest anti-inflammatory effect on type-1 and type-2 granulomas, respectively. Th1/Th2 cross-regulation was evident because endogenous Th2 cytokines inhibited type-1, whereas Th1 cytokines inhibited type-2 biased chemokines. These findings reveal a complex cytokine–chemokine regulatory network that dictates profiles of local chemokine expression during T cell–mediated granuloma formation.

The lung is the primary site of organ involvement in a number of granulomatous conditions that can be caused by a wide range of agents including infectious microorganisms, allergens and metals (1). The term “granuloma” fails to confer a sense of the rich histologic heterogeneity observed among these lesions, which can vary from simple mononuclear cell aggregates to florid necrotizing and even eosinophil-rich inflammations. We and others have demonstrated that hypersensitive-type granulomas are mediated by T cell–mediated immune mechanisms and T cell–derived cytokines appear to dictate the severity and histologic character of the lesions (2–4). Moreover, cytokine analyses indicate that granulomas can display polarized profiles consistent with predominant Th1 or Th2 cell involvement (5).

In addition to cytokines, granulomas are associated with a variety of chemokines (6, 7), which represent a family of molecules whose presumed function is to direct cellular movement. Chemokines participate during innate recognition stages of immunity and may help direct Th1 and Th2 cytokine-producing cells during the generation of adaptive immunity (8, 9). Furthermore, there is also considerable *in vitro* evidence that immune-related cytokines further capitalize on these effector molecules by regulating their expression and secretion. Chemokine expression by a variety of cultured cell types has been demonstrated to display positive and negative regulatory responses to cytokine stimulation

Address correspondence to: Stephen W. Chensue, M.D., Ph.D., Pathology and Laboratory Medicine 113, Veterans Affairs Medical Center, 2215 Fuller Road, Ann Arbor, MI 48105. schensue@med.umich.edu.

(10–15). It is unknown how such regulatory networks might operate *in vivo* during granuloma formation, and it is unclear how the current paradigm of Th1/Th2 biased immunity might influence such networks. In a previous report, we demonstrated different patterns of chemokine expression in well-defined models of Th1 and Th2 cytokine–mediated experimental lung granulomas, respectively, induced by mycobacterial and schistosomal Ag-coated beads (7). The different patterns of chemokine expression in these models were likely shaping the cellular composition and function of the lesions.

We hypothesized that differences in chemokine expression observed during adaptive immune pulmonary inflammation were the result of differential regulation by upstream Th1- and Th2-related cytokines. To test this hypothesis, we undertook a comprehensive analysis using *in vivo* neutralization of Th1 (interferon [IFN]-γ, interleukin [IL]-12)- and Th2 (IL-4, IL-10, IL-13)-related cytokines combined with quantitative transcript analysis of 16 chemokines induced in lungs during type-1 and type-2 Ag-bead granuloma formation. Our findings reveal a complex network in which type-1– and type-2–associated chemokine profiles are the result of cytokine-mediated amplification and inhibitory crossregulation by Th1- and Th2-related cytokines. Awareness of such networks will help design appropriate cytokine- and chemokine-directed therapies to help modulate granulomatous inflammatory conditions.

Materials and Methods

Animals

Female, CBA/J mice were obtained from Jackson Laboratories, Bar Harbor, ME. All mice were maintained under specific-pathogen free conditions and provided food and water *ad libitum*.

In Vivo Generation Type-1 and Type-2 Granulomas

Type-1 and type-2 secondary Ag-bead pulmonary granulomatous responses were generated in CBA mice as previously described (16). Briefly, mice were sensitized by subcutaneous injection of 20 μg *Mycobacteria bovis* purified protein derivative (PPD; Department of Agriculture, Veterinary Division, Ames, IA) incorporated in to 0.25 ml complete Freund's adjuvant (CFA, product number F-5881; Sigma, St. Louis, MO) or 3,000 *Schistosoma mansoni* eggs suspended in 0.5 ml phosphate-buffered saline (PBS). Fourteen to sixteen days later, PPD- and schistosome egg–sensitized mice were respectively challenged by tail vein with 6,000 Sepharose 4B beads (in 0.5 ml PBS) covalently coupled to PPD or to *S. mansoni*–soluble schistosome egg antigens (SEA) obtained from the World Health Organization, Geneva, Switzerland.

At designated intervals following challenge, lungs were removed after perfusion with cold isotonic buffer, then placed into RNAase inhibitor solution (RNAlater; Ambion, Austin, TX) before RNA extraction.

Assessment of Granuloma Cytokine Production

Granulomas were collected from bead-challenged lungs and cultured as previously described (5). Supernates were collected at 48 h and assayed for cytokine levels. Murine IFN-γ and IL-4, -10, -12, and -13 were measured by standard enzyme-linked immunosorbent assay (ELISA) using commercially available reagents and standards (R&D Systems, Minneapolis, MN; and PharMingen, San Diego, CA); sensitivities ranged from 15–50 pg/ml. In addition, aqueous lung extracts were prepared and endogenous cytokines measured by ELISA, then normalized to lung protein as previously described (7).

Antibodies and Treatment Regimen

Polyclonal anti-murine IFN-γ IL-10, IL-12, and IL-13 antisera were prepared by monthly immunizations of rabbits with the respective recombinant cytokines emulsified with CFA. Direct ELISA was used to determine antibody titers and specificity. Antibodies were used when titers reached 1:1,000,000 in direct ELISA, and if found specific when tested against a battery of recombinant murine cytokines that included tumor necrosis factor (TNF)-α, IL-1-α/β, IL-2, IL-4, IL-5, IL-10, IL-12, IL-13, monocyte chemotactic protein (MCP)-1, and macrophage inflammatory protein (MIP)-1α. *In vitro* neutralizing activity of anti–IFN-γ was determined by its capacity to block IFN-γ–mediated induction of macrophage IA antigen expression. Neutralizing activity of anti–IL-10 was determined by its capacity of to block IL-10–mediated suppression of macrophage IL-6 production. Anti–IL-12 neutralizing activity was assessed by inhibition of IL-12 stimulation of IFN-γ production by phytohemagglutinin-stimulated spleen cells. Anti–IL-13 neutralizing activity was confirmed by reversal of IL-13–mediated inhibition of macrophage nitric oxide production *in vitro*. Polyclonal IgG preparations were purified from antisera using protein A columns, dissolved in PBS, and then frozen at −50°C before use. Nonimmune rabbit IgG served as a control. Monoclonal rat anti-murine IL-4 was prepared from the 11B11 hybridoma line, grown in serum-free culture medium, and purified by immunoaffinity chromatography. This preparation showed no cross-reactivity with IL-13. Rat IgG served as a control. Neutralizing activity of anti–IL-4 was determined by inhibition of the IL-4–driven growth of CT.4S cells.

Groups of mice were administered Abs intraperitoneally (10 mg polyclonal IgG or 2 mg monoclonal IgG) or corresponding control IgG 30 min before challenge with Ag-coated beads, and then lungs were analyzed for chemokine transcript expression 2–4 d later.

Real Time RT-PCR Analysis of mRNA

Poly (A) pure mRNA was isolated from lung tissue using Poly(A)-Pure mRNA isolation kits (Ambion). The samples were each tested for contaminating genomic DNA by PCR analysis. Any contaminated sample was treated with DNAase until determined to be pure. Each mRNA sample of ~ 1 μg was reverse-transcribed in a 20-μl reaction in a PCR reaction-tube using Reverse Transcription System kits (Promega, Madison, WI). Four separate reactions were conducted to minimize variability between tubes. The products from each reaction tube were pooled to make one cDNA sample. ABI PRISM 7000 Sequence Detection System (Applied Biosystems, Foster City, CA) was used for real-time PCR analysis. For the current study, comparative CT method recommended by the manufacturer (Applied Biosystems) was adopted with glyceraldehyde phosphate dehydrogenase (GAPDH) as endogenous reference transcript, and primer-probed sets were designed with manufacturer's software. Primer and probe sequences for the 16 target chemokines and GAPDH are presented in Table 1. In all cases, the thermal cycling condition was programmed according to the manufacturer's instructions. Transcript levels were expressed as arbitrary units (AU) and were calculated as previously described (17). Briefly, AU were calculated from the fluorescence amplication factor as measured by the real-time PCR fluorescent detection unit. The original gene copy number (Co) is related to fluorescence of the generated signal as follows: $Co = F \times E^{-1} \times I \times 2^{-n}$, where F is an arbitrary conversion constant, E^{-1} is amplification efficiency constant (approximately =1 for manufacturer's real-time primers sets), I is the fluorescent intensity reading, and n is the amplification cycle number. Hence, $F \times E^{-1} \times I \times 2^{-n}$ constitutes an arbitrary measure of original copy number that is directly related to the fluorescent product and inversely related to cycle number. Because E is roughly equivalent for the various primer sets, the expression levels among genes are comparable at orders of magnitude.

Statistics

The Student's *t* test was used for comparison of control and treated groups. Values of *P* greater than or equal to 0.05 were considered to indicate lack of significance. In depletion studies, statistical analysis was performed for every chemokine transcript analysis. Statistically significant changes were generally observed when transcript levels were enhanced by 2-fold or more or decreased by more than 35%.

Results

Temporal Chemokine Transcript Profiles during Type-1 (Mycobacterial) and Type-2 (Schistosomal) Antigen-Bead Pulmonary Granuloma Formation

We previously reported that synchronous type-1 (mycobacterial) and type-2 (schistosomal) Ag bead granulomas displayed characteristic chemokine expression profiles (7). That study used a semiquantitative method for transcript analysis, which had a limited capacity to discern differences among high copy number transcripts. As part of the present study, we analyzed the expression of 16 chemokines in individual lungs using quantitative real-time, reverse transcriptase PCR, which is a more precise indicator of transcript levels. As shown in Figure 1, distinct patterns of chemokine transcript expression were identified using this approach. The CXCL chemokines, CXCL5 (LIX), CXCL2 (MIP-2), CXCL11 (I-TAC), CXCL10 (IP-10), and CXCL9 (MIG), as well as the CCL chemokines CCL3 (MIP-1α) and CCL4 (MIP-1β), were biased to the type-1 response, and the greatest expression occurred during the rapid growth phase of the lesion (1–3 d). Transcripts for CCL7 (MCP-3), CCL12 (MCP-5), CCL11 (eotaxin), and CCL17 (TARC) showed biased expression in the type-2 response. Interestingly, the type-2 bias of TARC expression was not discerned in our previous analysis, likely because this represents a high copy number transcript in both types of responses. CCL2 (MCP-1), CCL8 (MCP-2), and CCL1 (TCA-3) also showed trends to a type-2 bias, but overall these were expressed in both types of responses. In contrast to our previous study, we did not observe a clear type-1 bias of XCL1 (lymphotactin), but we did confirm that this chemokine was associated with the mid and late stages of lesion development. In terms of highest levels of expression (i.e., 2,000 AU or more), MIP-2, I-TAC, IP-10, MIG, MIP-1α, MIP-1β, MCP-1, and TARC dominated on Days 1–2 in the type-1 response. By Day 3, only MIP-1β, MIG, MDC, and TARC were expressed in this range, and by Day 8 only MDC persisted as a high copy number transcript. In the type-2 (SEA) response, MIP-1α, MCP-1, MCP-3, eotaxin, and TARC were at high copy number on Days 1–2. On Days 3–4, MIP-1β, MCP-2, MDC, and TARC were the dominant transcripts; and similar to the type-1 response, MDC persisted in this range by Day 8. Of the chemokine transcripts examined, the strongest signals were obtained for MDC, TARC, and MIG in the type-1 response and MDC, TARC, and MCP-3 in the type-2 response. Thus, MDC and TARC, ligands for CC-chemokine receptor 4 (CCR4), were expressed in both responses, and one or both were present at nearly all stages of the response. Figure 2 shows the temporal expression of these dominant transcripts plotted on a single scale.

Cytokine Depletions Exert Different Effects on Chemokine Transcript Expression during Type-1 (Mycobacterial) and Type-2 (Schistosomal) Antigen-Bead Pulmonary Granuloma Formation

We next tested the potential influence of cytokines in dictating the spectrum of chemokines produced during type-1 and type-2 granuloma formation. The targeted cytokines, IFN-γ, IL-4, IL-10, IL-12, and IL-13, were chosen based upon their known expression in these models and their potential regulatory function (5, 18–20). Figure 3 shows the temporal expression of these cytokines in whole lung extracts as well as in isolated and cultured granulomas during an 8-d time course. In whole lung extracts, background expression of cytokines was detectable even in naive lungs (dashed lines) and bead challenge increased

levels in both responses except for IL-4, which increased by 2-fold only at 4 d in the type-2 response. The lung extracts suggested some degree of biased expression, but this was more clearly revealed when granulomas were isolated and cultured. As we have previously reported, IFN-γ was biased to the type-1 (PPD), whereas IL-4 and IL-13 were biased to the type-2 (SEA) response. Surprisingly, IL-10 was produced by both lesion types, as was IL-12 (p70 heterodimer), though there was a trend to earlier production in the type-1 response. Both extract and culture results indicated that the type-1 response began active cytokine production on Days 1 and 2, whereas the type-2 response was more pronounced on Days 2 and 4.

To explore the relationship of chemokine expression to the above cytokines, mice were treated with neutralizing anti-cytokine antibodies as described in Materials and Methods, and then lungs were analyzed for chemokine transcript expression. Analysis was performed on Days 2–3 for the type-1 model and on Days 3–4 for the type-2 because cytokine production generally peaked later in the latter. For cytokine depletion analysis, anticytokine antibody preparations included anti–IFN-γ, anti–IL-12, anti–IL-4, anti–IL-10, and anti–IL-13; the *in vivo* efficacy of each of these preparations has been previously reported (18–20).

Effect of IFN-γ depletion—Figure 4 shows the effect of *in vivo* IFN-γ depletion on the levels of chemokine transcripts produced during the type-1 (PPD) and type-2 (SEA) responses. To consolidate and simplify the presentation, the data are normalized to show positive (fold-increases) or negative (percent decreases) changes from control IgG-treated animals. Parametric statistical analysis of all raw data indicated that significant changes were generally those with < 2-fold increase or < 35% decrease. *Asterisks* indicate significant changes and *dashed lines* are included only as a reference points. *Insets* show the effect of the treatment on granuloma inflammatory area on Day 4. Figure 4A demonstrates that in the type-1 PPD response, anti–IFN-γ treatment significantly reduced transcript levels for 10 of 16 chemokines. The Day 2 transcript reductions were associated with a 41% decrease in average granuloma inflammatory area by Day 4. Thus, it appeared that IFN-γ was supporting the expression of a number of type-1–biased chemokines, including LIX, MIP-2, I-TAC, IP-10 MIG and MIP-1β. The IFN-γ–dependence of I-TAC, IP-10, and MIG is fully consistent with their reported *in vitro* characterization (12, 21). In addition, lymphotactin and MCP-2, -3, and -5 were reduced by anti–IFN-γ treatment.

Figure 4B shows that type-2 (SEA) inflammation was exacerbated by anti–IFN-γ treatment as others and we have previously reported (19, 22). This exacerbation was associated with augmented expression of the higher copy number transcripts, MCP-2, MCP-3, MDC, and TARC. Thus, these transcripts were subject to negative regulation by endogenous IFN-γ, suggesting that Th2-related cytokines were mainly responsible for their induction. This apparent inhibitory influence of IFN-γ on dominant chemokines expressed during the type-2 response provides further explanation for the reported crossregulatory effect of this cytokine in the granulomatous response to schistosome egg Ags (22, 23). Interestingly, even the weakly expressed I-TAC, IP-10, and MIG transcripts were positively regulated by IFN-γ in the type-2 response, indicating their strong IFN-γ dependence. There was also a trend for IFN-γ depletion to reduce lymphotactin transcripts, but this just fell short of significance.

Effect of IL-12 depletion—Anti–IL-12 treatment abrogated 6 of 16 chemokine transcripts in the type-1 PPD response (Figure 5A). These included several of those that were also reduced by IFN-γ depletion, including I-TAC, IP-10, MIG, and MCP-2, supporting the known link between IL-12 and IFN-γ. Unlike IFN-γ depletion, IL-12 depletion reduced MIP-1α and MCP-1 transcript levels, but had no effect on LIX, MIP-2, MIP-1β, or lymphotactin. IL-12 depletion caused only a 14% decrease in the inflammatory area, suggesting that the affected chemokines were not essential to ultimately establish a

lesion; however, shifts in rate of granuloma formation or cell composition cannot be ruled out.

IL-12 depletion had an opposite effect on the type-2 response, enhancing 9 of 16 chemokine transcripts (Figure 5B). Unexpectedly, this was not associated with augmented granuloma formation as observed with IFN-γ depletion. Unlike with IFN-γ depletion, TARC was not included among the enhanced group. In addition, MIP-1α and MIP-1β were among the enhanced group; chemokines generally more biased to the type-1 response. Thus, the lack of exacerbated inflammation may be related to differences in the spectrum of enhanced chemokine transcripts as discussed later.

Effect of IL-10 depletion—Anti–IL-10 treatment had no significant effect on overall granuloma inflammatory area and marginally affected only 4 of 16 chemokines in the type-1 response (Figure 6A). Augmentations of MIP-1α and MIP-1β were observed, suggesting that IL-10 was a negative regulator and opposed the effect of IFN-γ and IL-12. In contrast, MCP-2 and TARC declined, suggesting that IL-10 supported their expression. In the type-2 response, IL-10 depletion caused a significant reduction in transcripts for only MCP-1, and this effect was associated with no significant change in granuloma sizes (Figure 6B). Thus overall, IL-10 had relatively limited regulatory effect on local chemokine transcript expression.

Effect of IL-13 depletion—Figure 7 demonstrates the effect of IL-13 depletion on chemokine transcripts. In the type-1 response, the treatment augmented I-TAC, IP-10, and MIG, thus IL-13 was a negative regulator of these chemokines and opposed IFN-γ and IL-12 (Figure 7A). However like IFN-γ, it seemed to support MCP-2 and MCP-3, although marginally. The latter finding conflicts with our previous study, likely because at that time optimal sampling times were unknown and quantitative transcript analysis was not used (20). In addition, it was identified as a significant contributor to Eotaxin, MDC, and TARC expression. Despite these changes in chemokine transcript expression, lesion sizes were unchanged, possibly because negative and positive regulatory effects neutralized each other or ultimate effects on protein expression were negligible.

In contrast to the PPD response, IL-13 is produced in greater amounts in the type-2 response, and depletion caused significant reductions in inflammation as well as in 7 of 16 chemokine transcripts (Figure 7B). Decreases were observed for MIP-1β, MCP-1, MCP-2, MCP-3, eotaxin, TARC, and CCL1 (TCA-3), suggesting that at least some of these chemokines were contributing to the type-2 response.

Effect of IL-4 depletion—Interleukin-4 is largely produced during the type-2 SEA response, and we have previously demonstrated this Th2-related cytokine to positively regulate MCP-1 and MCP-3 *in vivo* (20, 24). Figure 8 shows that anti–IL-4 treatment caused nearly a 40% decrease in granuloma size, which was associated with significant declines in 9 of 16 chemokine transcripts. Similar to IL-13, IL-4 supported MIP-1β, MCP-1, MCP-2, MCP-3, eotaxin, TARC, and CCL1 (TCA-3). In addition, it supported MCP-5 and MDC.

Interleukin-4 is produced negligibly in the type-1 (PPD) response, and its depletion did not significantly alter the gross degree of inflammation. Despite this, endogenous IL-4 was found to negatively influence LIX, MIP-2, and MIP-1α, and to positively regulate a similar complement of chemokine transcripts as it did in the type-2 response, including MCP-2, -3, and -5 as well as MDC and TARC (data not shown). Thus, this latter group of chemokines displayed a significant positive correlation to the Th2-related cytokines

Table 2 summarizes the regulatory influence of the studied cytokines in the two models. Taken together, the findings demonstrate that endogenous cytokines have both positive and negative regulatory effects on chemokine expression during the course of mycobacterial (type-1) and schistosomal (type-2) granuloma formation. The ultimate pattern of chemokines expressed is likely dependent on the net effect of these regulatory signals.

Discussion

The present study was undertaken to test the hypothesis that differences in chemokine expression observed during adaptive immune pulmonary inflammation were the result of differential regulation by upstream Th1- and Th2-related cytokines. Because our study used real-time quantitative transcript analysis, we initially wished to determine if our previously reported observations regarding type-1 and type-2 chemokine profiles could be substantiated and extended using this new method. Indeed, the majority of our previous observations were confirmed. In addition, we were able to better discern temporal expression and relative differences in copy numbers as well as reveal previously undetected greater expression of CCL17 (TARC) transcripts during type-2 (SEA) granuloma formation. We believe transcript monitoring is a reasonable approach to study chemokine dynamics because our previous study showed good correlation of transcript and protein expression (7). This approach proved highly effective in revealing intriguing and subtle relationships of chemokine and cytokine expression. The targeted cytokines, IFN-γ, IL-4, IL-10, IL-12, and IL-13, were chosen on the basis of their demonstrable local production and their established roles in Th1 and Th2 immune responses. As discussed below, all participated to a greater or lesser degree in shaping local chemokine expression.

The type-1 (PPD) response displayed biased expression of all CXCL chemokines examined, including CXCL2 (MIP-2), 5 (LIX), 9 (MIG), 10 (IP-10), and 11 (I-TAC) and the CCL chemokines, CCL3 (MIP-1α) and CCL4 (MIP-1β). Other than LIX, all were among the "high copy number" transcript group. This pattern fits the emerging concept of a "type-1" cluster of cytokines/chemokines coexpressed with IFN-γ and associated with NK cells, CD8+ T cells, and Th1 cells. Indeed, our study indicated strong dependence and temporal correlation of all of these chemokine transcripts with the type-1–associated cytokines IFN-γ and IL-12. Interestingly, only IFN-γ depletion reduced inflammation and correspondingly affected a broader scope of chemokines, also causing reductions in CCL8 (MCP-2), CCL7 (MCP-3), CCL5 (MCP-5), and (XCL1) lymphotactin. In our previous study using semiquantitative RNA analysis we were unable to demonstrate the broad influence of IFN-γ likely due to the lower sensitivity of that method (7). Although it is tempting to infer that the additionally reduced chemokines were critical for the inflammation, this might be simplistic because IFN-γ likely affects other proinflammatory elements such as cellular adhesion and oxygen metabolites. Our findings also indicated that IL-12 and IFN-γ have some independent functions promoting different chemokines, and that IFN-γ production was not wholly dependent on IL-12, likely due to other inducing factors such as IL-18 (25).

In the type-1 response, endogenous IL-10, IL-13, and IL-4 had both positive and negative regulatory effects. In general, all of the above-mentioned type-1–biased chemokines were negatively regulated by these cytokines, and surprisingly, each affected different chemokines. IL-10 mostly tempered CCL3 (MIP-1α) and CCL4 (MIP-1β), whereas IL-13 limited CXCL9 (MIG), 10 (IP-10), and 11 (I-TAC), and IL-4 reduced CXCL2 (MIP-2) and CXCL5 (LIX) transcript expression. Differential regulation of CCL3 (MIP-1α) and CCL4 (MIP-1β) by IFN-γ, IL-4, and IL-10 was reported for endotoxin-stimulated macrophages (10). We now provide evidence for differential cytokine crossregulation *in vivo*. Although the individual treatments did not significantly affect the degree of inflammation, we

previously demonstrated that combined IL-4 and IL-13 depletion significantly exacerbates type-1 granuloma formation (20).

Although IL-10, IL-13, and IL-4 downregulated the type-1–biased chemokine transcripts, they had positive effects on unbiased and normally type-2–biased chemokines. For example, MCP-2 (CCL8) was the only transcript that was enhanced by all of the cytokines examined, but IFN-γ and IL-12 were clearly the dominant positive stimulants during the type-1 response. Similarly, IFN-γ and IL-4 both promoted MCP-3 and MCP-5, further indicating that not all chemokines are subject to opposing influences. In contrast, eotaxin, MDC, and TARC were promoted only by IL-13, IL-4, or IL-10. The latter indicated that despite their low levels of expression in the type-1 response, the type-2–related cytokines, IL-13 and IL-4, were influencing the chemokine milieu, and IL-10, although not strictly a type-2 cytokine, was likewise promoting “type 2” chemokines. It should be noted that although our study did not address potential synergistic effects, such interactions are likely. The apparent biased expression of some chemokines may be in part due to contributing synergizing cytokines such as TNF-α (19, 22). We have previously demonstrated that TNF-α appears to promote several chemokines *in vivo* (7).

Our cytokine depletion analysis of the type-2 (SEA) response further revealed the existence of a dynamic cytokine–chemokine crossregulatory network. As we and others have previously reported, IFN-γ depletion exacerbated type-2 granulomatous inflammation (19, 22). This was associated with significant increases in CCL8 (MCP-2), CCL7 (MCP-3), CCL22 (MDC), and CCL17 (TARC). Further attesting to their IFN-γ dependence, the minor component of “type-1” chemokine transcripts, CXCL9 (MIG), 10 (IP-10), and 11 (I-TAC), were virtually eliminated. Thus, whereas IFN-γ was a major proinflammatory mediator in the type-1 granuloma, it served as a background counter-regulatory agent in the type-2 response. Of significant interest was the role of IL-12 in the type-2 lesion. Like IFN-γ, it had a counter-regulatory role, and its depletion augmented a broad spectrum of chemokine transcripts, including CCL3 (MIP-1α), CCL4 (MIP-1β), CCL2 (MCP-1), CCL8 (MCP-2), CCL7 (MCP-3), CCL12 (MCP-5), CCL11 (eotaxin), CCL22 (MDC), and CCL1 (TCA-3). Paradoxically, and unlike IFN-γ depletion, anti–IL-12 treatment did not cause a demonstrable increase in granuloma size, which may relate to the different spectrum of affected chemokines. Unlike IFN-γ neutralization, anti–IL-12 treatment concurrently increased transcripts for type-1–biased CCR1 ligands, CCL3 (MIP-1α), and CCL4 (MIP-1β), but did not enhance the type-2–biased chemokine, TARC (CCL17). The latter, being the dominantly expressed type-2 chemokine, may be a major proinflammatory signal. In addition, the type-1–biased ligands may act as crossregulatory receptor antagonists (26, 27). We specifically demonstrated that CCR1 ligation inhibited type-2 granuloma formation (28). Thus, any proinflammatory effects of the CCR2 and CCR3 ligands might be neutralized by concomittant augmentation of CCR1 ligands, resulting in no net change in type-2 inflammation. These different effects of IFN-γ and IL-12 blockade might have therapeutic implications. For example, attempts to neutralize IFN-γ to control Th1-domininant inflammatory conditions could have possible immunocompromising effects such as tuberculosis reactivation and potential exacerbation of allergic inflammation. However, targeting of IL-12 may provide anti-inflammatory benefit without as serious counter-regulatory effects.

Using repeated anti–IL-10 treatments, Boros and co-workers demonstrated a clear regulatory role for IL-10 in the inductive phase of the response to schistosome eggs (29). In our type-2 bead lesion, which represents an elicitation phase response, we observed only modest changes in the chemokine response manifest as increased CCL2 (MCP-1) transcript expression. This was consistent with our observation that IL-10 depletion did not affect inflammation, as well as with our previous report indicating that the major effect of IL-10

during the elicitation phase was detectable in draining lymphoid tissues and not at the site of inflammation (19). In contrast to IL-10, IL-13 and IL-4 had clear proinflammatory roles in type-2 granuloma formation. These cytokines promoted expression of a similar spectrum of chemokine transcripts, although that for IL-4 was broader, providing an explanation for the greater suppressive effect of IL-4 depletion. The broader effect of IL-4 may relate to its capacity to bind both IL-4 and IL-13 receptors, whereas IL-13 can only signal through its own receptor (30). The chemokine transcripts promoted by these cytokines included CCL4 (MIP-1β), CCL2 (MCP-1), CCL8 (MCP-2), CCL7 (MCP-3), CCL12 (MCP-5), CCL11 (eotaxin), CCL22 (MDC), CCL17 (TARC), and CCL1 (TCA-3). Of these, only CCL4 was classed among "type-1"–biased chemokines based upon our initial survey, and its promotion by both Th1- and Th2-related cytokines indicates that it is not limited to type-1 responses. This finding also provides further evidence for the notion that despite their similarity, CCL3 (MIP-1α) and CCL4 (MIP-1β) are independently expressed or regulated (10).

Of the many findings provided by our *in vivo* study, special mention should be made regarding CCL22 (MDC) and CCL17 (TARC). Both of these chemokines are ligands for the CCR4 receptor (31, 32) and have been associated with Th2-mediated hypersensitivity responses (33, 34). Our study showed significant transcript levels in both types 1 and 2 granuloma models, although CCL17 (TARC) was type-2 biased. We consistently showed that IL-13 enhanced CCL17 (TARC) transcripts and IL-4 enhanced CCL22 (MDC) and CCL17 (TARC) in both granuloma models. This finding is fully consistent with *in vitro* studies (32, 34), and supports these chemokines as important participants in Th2 cytokine–mediated responses. However, CCL22 (MDC) can be elicited by cytokines such as IL-1 and TNF-α (35), which are produced during the type-1 (PPD) response, and would explain the unbiased nature of MDC expression. Germane to this is our finding that unlike *in vitro*–generated Th cell clones, CCR4 was a major chemokine receptor expressed by both IL-4– and IFN-γ–producing CD4+ T cells generated *in vivo* during Ag-bead granuloma formation (17). Thus, MDC and TARC may not necessarily be recruiting only Th2-restricted cells. Consequently, the net "polarized" state may reflect more on Th cell frequency and cross-regulatory signaling.

In summary, although our *in vivo* study has interpretive limitations regarding actual translated protein levels and specific sites of chemokine synthesis within granulomatous lungs, it provides the first comprehesive analysis of cytokine-mediated regulation of chemokine expression during type-1 and type-2 models of chronic inflammation. The following findings emerge from this study: (*i*) chemokine expression is subject to crossregulation by Th1- and Th2- related cytokines; (*ii*) enhancement or decrease in chemokine expression will not necessarily result in changes in inflammation unless critical chemokines or critical thresholds are affected; (*iii*) chemokines are differentially regulated by cytokines *in vivo*; (*iv*) there is profound expression of CCR4 agonists, during granuloma formation, which are clearly augmented by IL-4 and IL-13; and (*v*) biased patterns of chemokine expression during the adaptive immune response can be related to the cytokine milieu. Such *in vivo* studies will be relevant to current efforts to target cytokine and chemokines in pulmonary disease.

Acknowledgments

This work was supported by NIH-NIAID grant AI43460 and in part by the Department of Veterans Affairs. Schistosome life stages or materials for this work were supplied through NIH-NIAID contract NO1-AI-55270.

Abbreviations

Ags antigens

CCL	CC chemokine ligand
CFA	complete Freund's adjuvant
CXCL	CXC chemokine ligand
ELISA	enzyme-linked immunosorbent assay
IFN-γ	interferon-γ
IL	interleukin
MCP	monocyte chemotactic protein
MIP	macrophage inflammatory protein
PBS	phosphate-buffered saline
PPD	purified protein derivative of mycobacteria
SEA	schistosomal soluble egg antigen
TNF	tumor necrosis factor

References

1. Boros DL. Granulomatous inflammations. Prog. Allergy. 1978; 24:183–243. [PubMed: 351629]
2. Munk ME, Emoto M. Functions of T-cell subsets and cytokines in mycobacterial infections. Eur. Respir. J. Suppl. 1995; 20:668s–675s. [PubMed: 8590567]
3. Kunkel SL, Lukacs NW, Strieter RM, Chensue SW. Th1 and Th2 responses regulate experimental lung granuloma development. Sarcoidosis Vasc. Diffuse Lung Dis. 1996; 13:120–128. [PubMed: 8893380]
4. Boros DL. T helper cell populations, cytokine dynamics, and pathology of the schistosome egg granuloma. Microbes Infect. 1999; 1:511–516. [PubMed: 10603567]
5. Chensue SW, Warmington K, Ruth J, Lincoln P, Kuo MC, Kunkel SL. Cytokine responses during mycobacterial and schistosomal antigen-induced pulmonary granuloma formation: production of Th1 and Th2 cytokines and relative contribution of tumor necrosis factor. Am. J. Pathol. 1994; 145:1105–1113. [PubMed: 7977642]
6. Sadek MI, Sada E, Toossi Z, Schwander SK, Rich EA. Chemokines induced by infection of mononuclear phagocytes with mycobacteria and present in lung alveoli during active pulmonary tuberculosis. Am. J. Respir. Cell Mol. Biol. 1998; 19:513–521. [PubMed: 9730880]
7. Qiu B, Frait KA, Reich F, Komuniecki E, Chensue SW. Chemokine expression dynamics in mycobacterial (type-1) and schistosomal (type-2) antigen-elicited pulmonary granuloma formation. Am. J. Pathol. 2001; 158:1503–1515. [PubMed: 11290568]
8. Lu B, Rutledge BJ, Gu L, Fiorillo J, Lukacs NW, Kunkel SL, North R, Gerard C, Rollins BJ. Abnormalities in monocyte recruitment and cytokine expression in monocyte chemoattractant protein 1-deficient mice. J. Exp. Med. 1998; 187:601–608. [PubMed: 9463410]
9. Lo D, Feng L, Li L, Carson MJ, Crowley M, Pauza M, Nguyen A, Reilly CR. Integrating innate and adaptive immunity in the whole animal. Immunol. Rev. 1999; 169:225–239. [PubMed: 10450520]
10. Sherry B, Espinoza M, Manogue KR, Cerami A. Induction of the chemokine beta peptides, MIP-1 alpha and MIP-1 beta, by lipopoly-saccharide is differentially regulated by immunomodulatory cytokines gamma-IFN, IL-10, IL-4, and TGF-beta. Mol. Med. 1998; 4:648–657. [PubMed: 9848081]
11. Teran LM, Mochizuki M, Bartels J, Valencia EL, Nakajima T, Hirai K, Schroder JM. Th1- and Th2-type cytokines regulate the expression and production of eotaxin and RANTES by human lung fibroblasts. Am. J. Respir. Cell Mol. Biol. 1999; 20:777–786. [PubMed: 10101011]
12. Gasperini S, Marchi M, Calzetti F, Laudanna C, Vicentini L, Olsen H, Murphy M, Liao F, Farber J, Cassatella MA. Gene expression and production of the monokine induced by IFN-gamma (MIG), IFN-inducible T cell alpha chemoattractant (I-TAC), and IFN-gamma-inducible protein-10

(IP-10) chemokines by human neutrophils. J. Immunol. 1999; 162:4928–4937. [PubMed: 10202039]

13. Pype JL, Dupont LJ, Menten P, Van Coillie E, Opdenakker G, Van Damme J, Chung KF, Demedts MG, Verleden GM. Expression of monocyte chemotactic protein (MCP)-1, MCP-2, and MCP-3 by human airway smooth-muscle cells. Modulation by corticosteroids and T-helper 2 cytokines. Am. J. Respir. Cell Mol. Biol. 1999; 21:528–536. [PubMed: 10502563]
14. Lamkhioued B, Garcia-Zepeda EA, Abi-Younes S, Nakamura H, Jedrzkiewicz S, Wagner L, Renzi PM, Allakhverdi Z, Lilly C, Hamid Q, Luster AD. Monocyte chemoattractant protein (MCP)-4 expression in the airways of patients with asthma. Induction in epithelial cells and mononuclear cells by proinflammatory cytokines. Am. J. Respir. Crit. Care Med. 2000; 162:723–732. [PubMed: 10934112]
15. Fujisawa T, Kato Y, Atsuta J, Terada A, Iguchi K, Kamiya H, Yamada H, Nakajima T, Miyamasu M, Hirai K. Chemokine production by the BEAS-2B human bronchial epithelial cells: differential regulation of eotaxin, IL-8, and RANTES by TH2- and TH1- derived cytokines. J. Allergy Clin. Immunol. 2000; 105:126–133. [PubMed: 10629462]
16. Chensue SW, Warmington K, Ruth JH, Lukacs N, Kunkel SL. Mycobacterial and schistosomal antigen-elicited granuloma formation in IFN-gamma and IL-4 knockout mice: analysis of local and regional cytokine and chemokine networks. J. Immunol. 1997; 159:3565–3573. [PubMed: 9317156]
17. Chiu BC, Shang XZ, Stolberg VR, Komuniecki E, Chensue SW. Population analysis of CD4+T cell chemokine receptor transcript expression during in vivo type-1 (mycobacterial) and type-2 (schistosomal) immune responses. J. Leukoc. Biol. 2002; 72:363–372. [PubMed: 12149428]
18. Chensue SW, Ruth JH, Warmington K, Lincoln P, Kunkel SL. In vivo regulation of macrophage IL-12 production during type 1 and type 2 cytokine-mediated granuloma formation. J. Immunol. 1995; 155:3546–3551. [PubMed: 7561051]
19. Chensue SW, Warmington KS, Ruth JH, Lincoln P, Kunkel SL. Cytokine function during mycobacterial and schistosomal antigen-induced pulmonary granuloma formation. Local and regional participation of IFN-gamma, IL-10, and TNF. J. Immunol. 1995; 154:5969–5976. [PubMed: 7751640]
20. Ruth JH, Warmington KS, Shang X, Lincoln P, Evanoff H, Kunkel SL, Chensue SW. Interleukin-4 and -13 participation in mycobacterial (type-1) and schistosomal (type-2) antigen-elicited pulmonary granuloma formation: Multiparameter analysis of cellular recruitment, chemokine expression and cytokine networks. Cytokine. 2000; 12:432–444. [PubMed: 10857756]
21. Farber JM. Mig and IP-10: CXC chemokines that target lymphocytes. J. Leukoc. Biol. 1997; 61:246–257. [PubMed: 9060447]
22. Lukacs NW, Boros DL. Lymphokine regulation of granuloma formation in murine schistosomiasis mansoni. Clin. Immunol. Immunopathol. 1993; 68:57–63. [PubMed: 8513594]
23. Chensue SW, Warmington KS, Ruth J, Lincoln PM, Kunkel SL. Cross-regulatory role of interferon-gamma (IFN-gamma), IL-4 and IL-10 in schistosome egg granuloma formation: *in vivo* regulation of Th activity and inflammation. Clin. Exp. Immunol. 1994; 98:395–400. [PubMed: 7994903]
24. Shang XZ, Chiu BC, Stolberg V, Lukacs NW, Kunkel SL, Murphy HS, Chensue SW. Eosinophil recruitment in type-2 hypersensitivity pulmonary: granulomas source and contribution of monocyte chemotactic protein-3 (CCL7). Am. J. Pathol. 2002; 161:257–266. [PubMed: 12107110]
25. Ushio S, Namba M, Okura T, Hattori K, Nukada Y, Akita K, Tanabe F, Konishi K, Micallef M, Fujii M, Torigoe K, Tanimoto T, Fukuda S, Ikeda M, Okamura H, Kurimoto M. Cloning of the cDNA for human IFN-gamma-inducing factor, expression in *Escherichia coli*, and studies on the biologic activities of the protein. J. Immunol. 1996; 156:4274–4279. [PubMed: 8666798]
26. Loetscher P, Pellegrino A, Gong JH, Mattioli I, Loetscher M, Bardi G, Baggiolini M, Clark-Lewis I. The ligands of CXC chemokine receptor 3, I-TAC, Mig, and IP10, are natural antagonists for CCR3. J. Biol. Chem. 2001; 276:2986–2991. [PubMed: 11110785]
27. Marleau S, Griffiths-Johnson DA, Collins PD, Bakhle YS, Williams TJ, Jose PJ. Human RANTES acts as a receptor antagonist for guinea pig eotaxin in vitro and in vivo. J. Immunol. 1996; 157:4141–4146. [PubMed: 8892650]

28. Chensue SW, Warmington KS, Allenspach EJ, Lu B, Gerard C, Kunkel SL, Lukacs NW. Differential expression and cross-regulatory function of RANTES during mycobacterial (type 1) and schistosomal (type 2) antigen-elicited granulomatous inflammation. J. Immunol. 1999; 163:165–173. [PubMed: 10384113]

29. Boros DL, Whitfield JR. Endogenous IL-10 regulates IFN-gamma and IL-5 cytokine production and the granulomatous response in *Schistosomiasis mansoni*–infected mice. Immunology. 1998; 94:481–487. [PubMed: 9767435]

30. Hilton DJ, Zhang JG, Metcalf D, Alexander WS, Nicola NA, Willson TA. Cloning and characterization of a binding subunit of the interleukin 13 receptor that is also a component of the interleukin 4 receptor. Proc. Natl. Acad. Sci. USA. 1996; 93:497–501. [PubMed: 8552669]

31. Imai T, Baba M, Nishimura M, Kakizaki M, Takagi S, Yoshie O. The T cell-directed CC chemokine TARC is a highly specific biological ligand for CC chemokine receptor 4. J. Biol. Chem. 1997; 272:15036–15042. [PubMed: 9169480]

32. Andrew DP, Chang MS, McNinch J, Wathen ST, Rihanek M, Tseng J, Spellberg JP, Elias CG III. STCP-1 (MDC) CC chemokine acts specifically on chronically activated Th2 lymphocytes and is produced by monocytes on stimulation with Th2 cytokines IL-4 and IL-13. J. Immunol. 1998; 161:5027–5038. [PubMed: 9794440]

33. Gonzalo JA, Pan Y, Lloyd CM, Jia GQ, Yu G, Dussault B, Powers CA, Proudfoot AE, Coyle AJ, Gearing D, Gutierrez-Ramos JC. Mouse monocyte-derived chemokine is involved in airway hyperreactivity and lung inflammation. J. Immunol. 1999; 163:403–411. [PubMed: 10384142]

34. Terada N, Nomura T, Kim WJ, Otsuka Y, Takahashi R, Kishi H, Yamashita T, Sugawara N, Fukuda S, Ikeda-Ito T, Konno A. Expression of C–C chemokine TARC in human nasal mucosa and its regulation by cytokines. Clin. Exp. Allergy. 2001; 31:1923–1931. [PubMed: 11737045]

35. Rodenburg RJ, Brinkhuis RF, Peek R, Westphal JR, Van Den Hoogen FH, van Venrooij WJ, van de Putte LB. Expression of macrophage-derived chemokine (MDC) mRNA in macrophages is enhanced by interleukin-1beta, tumor necrosis factor alpha, and lipopoly-saccharide. J. Leukoc. Biol. 1998; 63:606–611. [PubMed: 9581805]

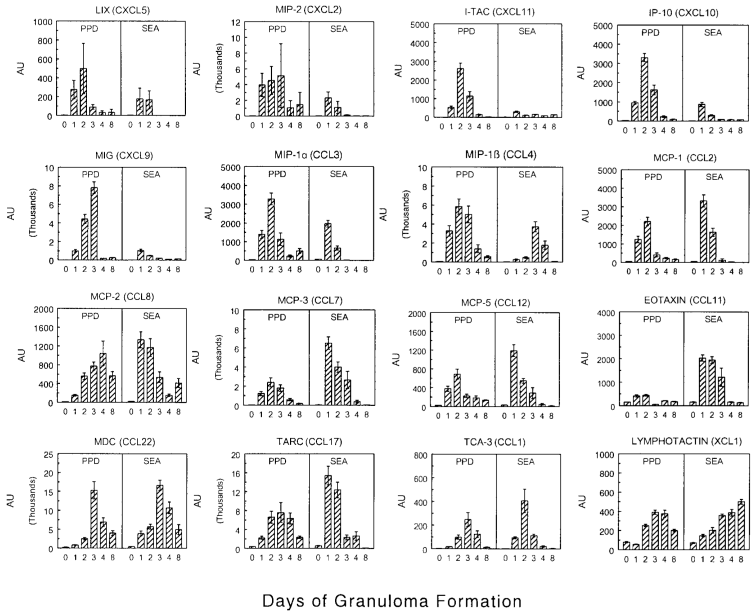

Figure 1.

Expression of chemokine receptor transcripts during synchronized type-1 (PPD) and type-2 (SEA) T cell–mediated granuloma formation as determined by real-time RT-PCR. *Bars* are mean arbitrary units (AU) ± SE derived from five to six individual lungs per point.

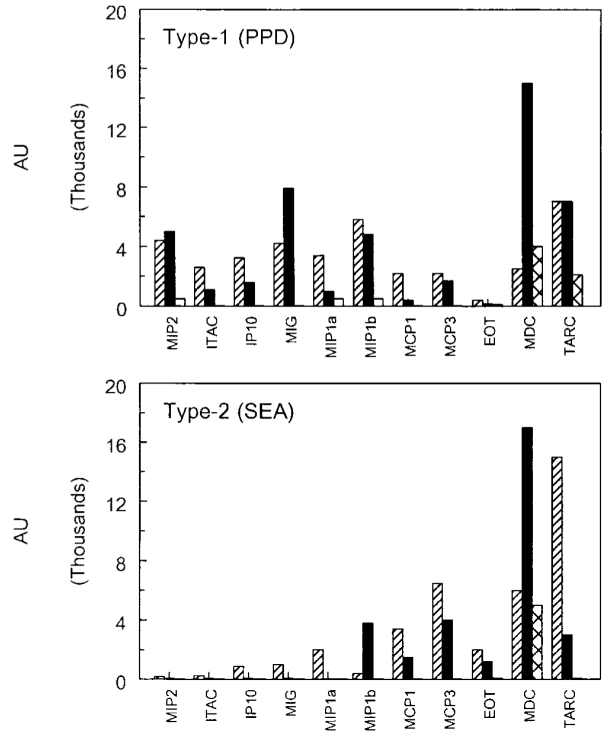

Figure 2.

Time course of expression of dominant chemokine transcripts during type-1 (PPD) and type-2 (SEA) T cell–mediated granuloma formation. *Bars* represent the maximum level of expression of dominant chemokine transcripts during the indicated time windows. *Striped bars*, 1–2 d; *solid bars*, 3–4 d; *hatched bars*, 8 d. Values are plotted on a common scale to show relative levels of expression.

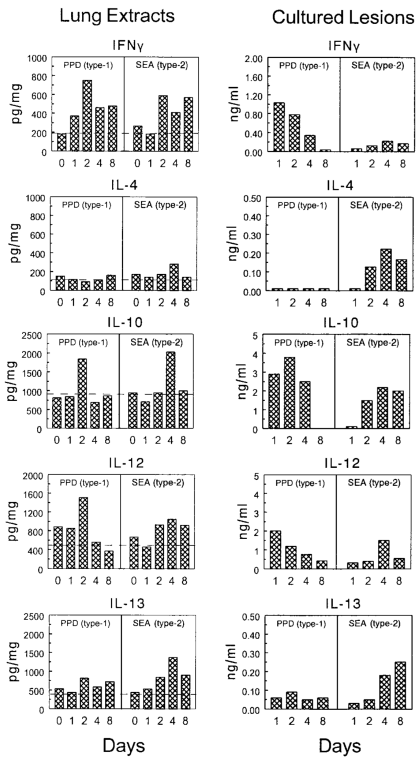

Figure 3.

Cytokine levels in whole lung extracts and cultured type-1 (PPD) and type-2 (SEA) Ag-bead lung granulomas. Aqueous lung extracts were prepared from 5–10 mice at each point, then assayed by ELISA for the indicated cytokines. Levels were normalized to total extracted lung protein. *Dashed lines* indicate levels in naive unchallenged lungs. In the right, cultured granulomas were isolated from 3–4 mice per day point and cultured (1,000/ml) for 48 h in the presence of either PPD or SEA antigens (5 μg/ml). Supernates were collected and assayed by ELISA in triplicate for the indicated cytokines. Data were derived from three separate experiments.

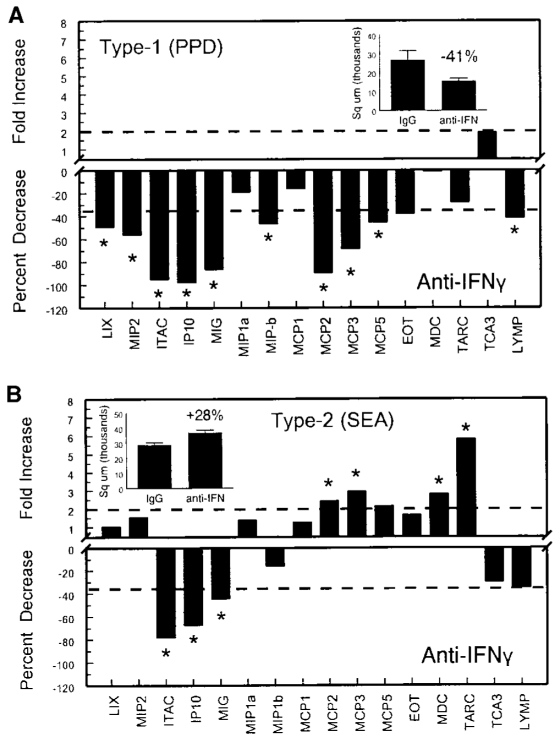

Figure 4.

Effect of anti–IFN-γ treatment on chemokine expression during type-1 (PPD) and type-2 (SEA) granuloma formation. *A*, type-1 (PPD) response; *B*, type-2 (SEA) response. *Upper sections* of charts indicate fold increase over control, and *lower sections* percent decrease from control as calculated from measured AU. Statistical analysis was performed on measured values (five separate lungs per control and treated groups). *Asterisks* indicate $P < 0.05$. *Dashed lines* demarcate zones of no statistically significant change. *Inset* shows average granuloma cross-sectional area on Day 4; indicated changes were significant at $P < 0.05$ unless marked NS.

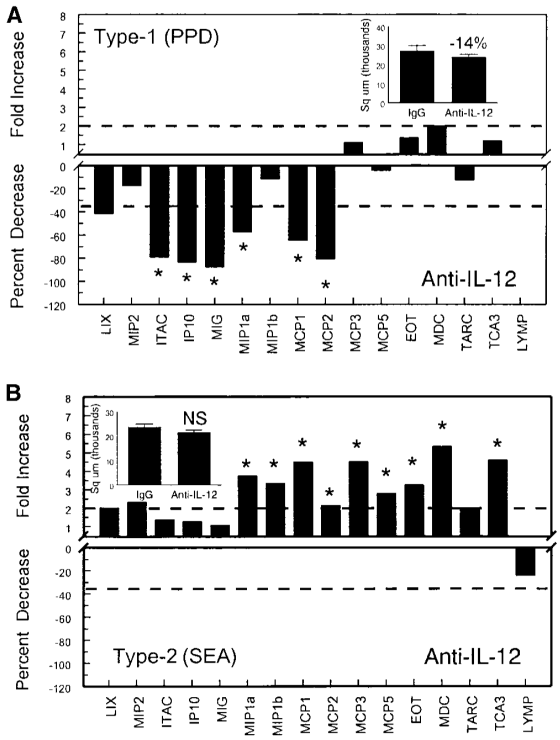

Figure 5.

Effect of anti–IL-12 treatment on chemokine expression during type-1 (PPD) and type-2 (SEA) granuloma formation. *A*, type-1 (PPD) response; *B*, type-2 (SEA) response. *Upper sections* of charts indicate fold increase over control, and *lower sections* percent decrease from control as calculated from measured AU. Statistical analysis was performed on measured values (five separate lungs per control and treated groups). *Asterisks* indicate $P < 0.05$. *Dashed lines* demarcate zones of no statistically significant change. *Inset* shows average granuloma cross-sectional area on Day 4; indicated changes were significant at $P < 0.05$ unless marked NS.

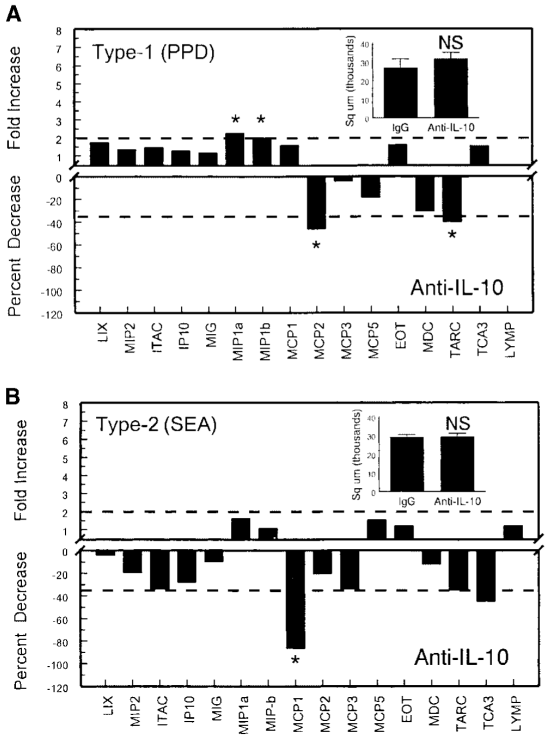

Figure 6.

Effect of anti–IL-10 treatment on chemokine expression during type-1 (PPD) and type-2 (SEA) granuloma formation. *A*, type-1 (PPD) response; *B*, type-2 (SEA) response. *Upper sections* of charts indicate fold increase over control, and *lower sections* percent decrease from control as calculated from measured AU. Statistical analysis was performed on measured values (five separate lungs per control and treated groups). *Asterisks* indicate $P < 0.05$. *Dashed lines* demarcate zones of no statistically significant change. *Inset* shows average granuloma cross-sectional area on Day 4; indicated changes were significant at $P < 0.05$ unless marked NS.

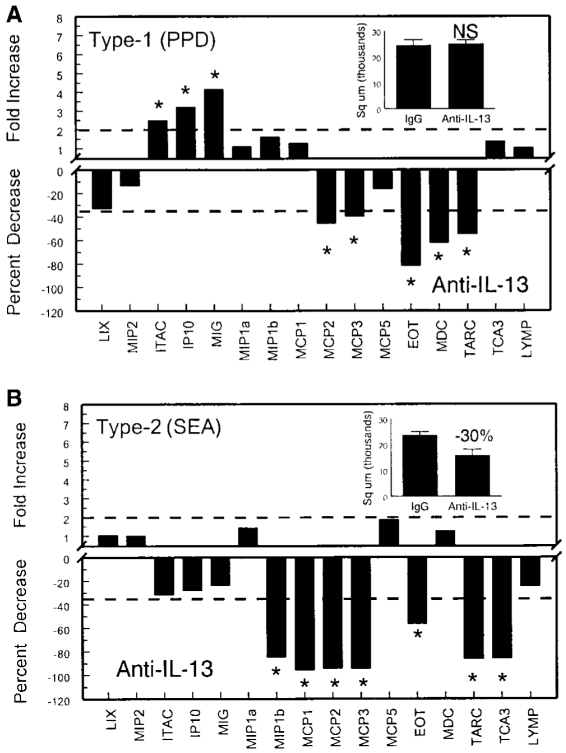

Figure 7.

Effect of anti–IL-13 treatment on chemokine expression during type-1 (PPD) and type-2 (SEA) granuloma formation. *A*, type-1 (PPD) response; *B*, type-2 (SEA) response. *Upper sections* of charts indicate fold increase over control, and *lower sections* percent decrease from control as calculated from measured AU. Statistical analysis was performed on measured values (five separate lungs per control and treated groups). *Asterisks* indicate $P < 0.05$. *Dashed lines* demarcate zones of no statistically significant change. *Inset* shows average granuloma cross-sectional area on Day 4; indicated changes were significant at $P < 0.05$ unless marked NS.

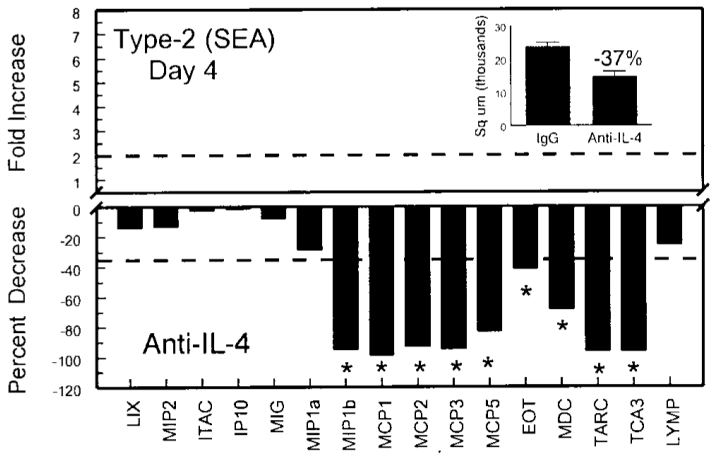

Figure 8.

Effect of anti–IL-4 treatment on chemokine expression during type-2 (SEA) granuloma formation. *Upper section* indicates fold increase over control, and *lower section* percent decrease from control as calculated from measured AU. Statistical analysis was performed on measured values (five separate lungs per control and treated groups). *Asterisks* indicate $P < 0.05$. *Dashed lines* demarcate zones of no statistically significant change. *Inset* shows average granuloma cross-sectional area on Day 4; indicated changes were significant at $P < 0.05$ unless marked NS.

TABLE 1

Chemokine probe and primer sequences

Chemokine	NCBI Sense	Probe (5′–3′)	Sense Primer (5′–3′)	Antisense Primer (5′–3′)
CXCL2 (MIP-2)	MMMIP2	CCCCACTGCGCCCAGACAGAAGT	AGCTTGAGTGTACGCCCC	TTGACCGCCCTTGAGAGTG
CXCL5 (LIX)	MMU27267	CTGCGGCAGCGTGAACAGCAAC	ATCTTGTCCACAATGAGCCTCC	TTGCGGCTATGACTGAGGAAG
CXCL9 (MIG)	M34815	CCTCACCAAGCTGGAGAGGCCCT	CTGAGGCTCACGTCACCAAGTC	GGCTCTAGGCTGACCCAAATG
CXCL10 (IP10)	MUSIP10	CATCCCAGCCACTTGAGCGAGGAC	TCAAGCCATGGTCCTGAGACAA	CGCACCTCCACATAGCTTACAG
CXCL11 (I-TAC)	AF178672	ACAGCAGAGGGTCAGGTTCCTGGC	CCTGGGAACGTCTGACTGTG	TCTGCAGCCTGGTAATACGTG
CCL4 (MIP-1β)	MUSMIP1X	CCAATGGGCTCTGACCCTCCC	CTTCTGTGCTCCAGGGTTCTC	GAGCAAAGACTGCTGGTCTCA
CCL8 (MCP2)	AB023418	CCCTTCGGGTGCTGAAAAGCTACG	GAAGCTGACTGGGCCAGATAAG	GCTTGGTCTGGAAAACCACAG
CCL11 (Eotaxin)	U26426	ATGAAGCCAAGTCCTTGGGCGA	TGACACTAACCCAGAGCCTAAG	CATAATGACTTCCAGTCCCATC
CCL12 (MCP5)	MMU50712	CTCACCGCATCTGGTCCAGCCAA	CTTCTATGCCTCCTGCTCATAGC	CGGACGTGAATCTTCTGCTTAAC
XCL1 (Lymphotactin)	MMU15607	ACTGCTGTGCTGGTGGACCTCTG	TGAAAGCAGCGATCAAGACTG	ACATTGTCCTGGAGGCTGTTAC
TaqMan predeveloped reaction kits (commercial sequences not provided by the manufacturer)				
CCL1 (TCA-3)				
CCL2 (MCP1)				
CCL3 (MIP-1α)				
CCL7 (MCP3)				
CCL17 (TARC)				
CCL22 (MDC)				
GAPDH				

TABLE 2

Summary of in vivo cytokine regulatory effects on chemokine transcript expression during type-1 (PPD) and type-2 (SEA) Ag-bead granuloma formation

Type-1 (Mycobacterial)						**Type-2 (Schistosomal)**				
Transcript:	IFN	IL-12	IL-10	IL-13	IL-4	IFN	IL-12	IL-10	IL-13	IL-4
LIX	pos	0	0	0	neg	0	0	0	0	0
MIP-2	pos	0	0	0	neg	0	0	0	0	0
ITAC	pos	pos	0	neg	0	pos	0	0	0	0
IP10	pos	pos	0	neg	0	pos	0	0	0	0
MIG	pos	pos	0	neg	0	pos	0	0	0	0
MIP1α	0	pos	neg	0	neg	0	neg	0	0	0
MIP-β	pos	0	neg	0	nd	0	neg	0	pos	pos
MCP1	0	pos	0	pos	nd	0	neg	pos	pos	pos
MCP2	pos	pos	pos	pos	pos	neg	neg	0	pos	pos
MCP3	pos	0	0	0	pos	neg	neg	0	pos	pos
MCP5	pos	0	0	0	pos	0	neg	0	0	pos
EOT	0	0	0	pos	0	0	neg	0	pos	pos
MDC	0	0	0	0	pos	neg	neg	0	0	pos
TARC	0	0	pos	pos	pos	neg	0	0	pos	pos
TCA3	0	0	0	0	0	0	neg	0	pos	pos
LYMP	pos	0	0	0	0	0	0	0	0	0

Am J Respir Cell Mol Biol. Author manuscript; available in PMC 2013 June 10.